

Article

Disturbance Observer-Based Tracking Controller for n -Link Flexible-Joint Robots Subject to Time-Varying State Constraints

Zhongcai Zhang ^{1,2,*}, Xueli Hu ² and Peng Huang ²¹ School of Artificial Intelligence, Nankai University, Tianjin 300350, China² School of Engineering, Qufu Normal University, Rizhao 276826, China; 17856858047@qfnu.edu.cn (X.H.); huang89553@qfnu.edu.cn (P.H.)

* Correspondence: zhangzc@qfnu.edu.cn

Abstract: This paper addresses the tracking control for an n -link flexible-joint robot system with full-state constraints and external disturbances. First, a nonlinear disturbance observer (NDO) is introduced to asymptotically estimate and suppress the influence of the related disturbances. Next, the constrained system under consideration is transformed into a new unconstrained system using state-dependent function (SDF) transformations. Subsequently, a NDO-based tracking controller that combines the backstepping method and filter technique is proposed in this work. Based on stability analysis, it can be proven that the tracking error converges to a predefined compact set, which can be arbitrarily small without violating the full-state constraints. Finally, simulation results are presented to demonstrate the validity of the suggested control algorithm.

Keywords: flexible-joint robots; nonlinear disturbance observer; state-dependent function; full-state constraints



Citation: Zhang, Z.; Hu, X.; Huang, P. Disturbance Observer-Based Tracking Controller for n -Link Flexible-Joint Robots Subject to Time-Varying State Constraints. *Electronics* **2024**, *13*, 1773. <https://doi.org/10.3390/electronics13091773>

Academic Editor: Manuel F. Silva

Received: 15 March 2024

Revised: 14 April 2024

Accepted: 2 May 2024

Published: 4 May 2024



Copyright: © 2024 by the authors. Licensee MDPI, Basel, Switzerland. This article is an open access article distributed under the terms and conditions of the Creative Commons Attribution (CC BY) license (<https://creativecommons.org/licenses/by/4.0/>).

1. Introduction

As a significant branch of robots, manipulators have evolved from rigid structures to flexible ones to meet the growing demands. Therefore, the studies on flexible-joint (FJ) robot systems have attracted wide attention [1–6]. Ref. [2] presented a comprehensive review of the mechanical design and synthesis of piezoelectric-actuated compliant micro positioning platforms based on the composition of flexible mechanisms. Ref. [3] proposed a dynamic modeling method for a multi-flexible-body robot system. Ref. [4] developed a nonlinear observer for an FJ manipulator to address the difficulty in measuring velocity signals. Ref. [5] analyzed the drive system and control strategy for a hyper-redundant continuous robot. In [6], an adaptive torque observer based on fuzzy inference was proposed for a permanent magnet synchronous machine (PMSM), and was further applied to an FJ manipulator.

The tracking control of flexible-joint (FJ) robots has indeed been a challenging and important area of research in control theory and engineering. The increasing order and nonlinear coupling characteristics of FJ robot systems have made the control particularly difficult [7–11]. Moreover, the introduction of an integral manifold approach has been significantly investigated in this field. By leveraging the accurate system modeling, the integral manifold approach facilitates the transformation of an FJ system into a rigid one, thereby reducing the design complexity [12,13]. Subsequently, a variety of advanced control methods, including backstepping control [14,15], PID control [16,17], sliding mode control [18,19], and others, have been introduced to address the control problems in FJ robots. In the presence of model uncertainty, adaptive control design plays a critical role in developing controllers that can effectively achieve the control objectives [20,21]. To enhance the system performance, adaptive control design often makes use of neural networks (NNs) and fuzzy systems, which possess universal approximation capabilities [22,23]. Ref. [24] proposed a unique adaptive neural network control technique for resolving the tracking

control problem for flexible-joint robots with random noises. In [25], an adaptive fuzzy control scheme was proposed under an event-triggered mechanism.

While the aforementioned methods are effective for FJ robots' tracking control, they may not adequately address the issue of tracking control in the presence of state constraints. For instance, when transporting goods, FJ manipulators must operate within the specified constraint zones to prevent crashes. To handle these constraints, robust control strategies for nonlinear systems, such as model predictive control [26,27] and set invariance notions [28,29] have been investigated. Subsequently, the use of barrier Lyapunov functions (BLFs) to handle the state constraints in nonlinear systems is becoming increasingly common [30–32]. An FJ robot's adaptive fuzzy tracking control with full-state constraints was proposed in [33]. Ref. [34] proposed an event-triggered control approach to deal with output constraints and make the system finite-time convergent. In addition, a new control approach for an FJ robot manipulator with full-state constraints was provided in [35], where the investigated constrained system was transformed into a new unconstrained system by applying state-dependent function transformations (SDFs).

With the advancement of robot technology in recent years, enhancing robot performance to attain higher accuracy and faster speeds without increasing costs has gained more attention. The greatest obstacle to achieving this goal is the constraints that disturbances impose. In practical control scenarios, interference can readily degrade the control performance. Disturbance observer (DO) is a widely utilized technique in most of the trajectory tracking control literature for dealing with time-varying external disturbances [36]. In [37], an adaptive neural control based on a DO was presented for n -link FJ robots. A sliding mode disturbance observer was designed for a nonlinear system in [38]. Ref. [39] introduced a new DO-based neural network integral sliding mode controller with output constraints, which combined the advantages of neural networks, disturbance observer, and integral sliding mode.

Until now, there have been limited studies addressing the n -link FJ robot manipulator systems with full-state constraints and external disturbances. To address these challenges, this paper introduced a DO-based nonlinear tracking controller for the considered systems. Initially, the original dynamic equations are transformed into a chained system and the external disturbances are estimated by the introduced nonlinear disturbance observer. Subsequently, the system with full-state constraints is transformed into an unconstrained system by the SDF transformation, which can simplify the controller design. Using the backstepping method as well as the filter technique, the nonlinear anti-disturbance tracking controller is obtained. The key contributions of this paper can be outlined as follows:

- (I) The proposed method offers a wider range of applications. Compared with the single-link FJ manipulator in [35,40], the studied system in this paper belongs to a class of complex MIMO systems, which means that the proposed control method has a wider application range.
- (II) The proposed method is easier to implement. Compared with the BLF-based method [33], the proposed state-constrained method removes the feasibility conditions, which broadens the range of acceptable initial values and relaxes the requirements for control parameters.
- (III) To address the issue of external disturbances, an NDO is incorporated for the real-time estimation of disturbances. In the controller design phase, filter techniques are employed to efficiently mitigate the problem of differential explosion resulting from the repeated differentiation of virtual control inputs.
- (IV) Through simulation results, we demonstrate the effectiveness and robustness of the proposed method. The proposed method ensures the effective control performance, and enhances the system's anti-disturbance capability. In addition, the system states do not violate the constraints under the design control strategy. And the tracking error can be made arbitrarily small by properly adjusting the design parameters.

The rest of this paper is organized as follows. Section 2 gives the problem formulation and preliminaries. DO-based control design and stability analysis are presented in Section 3. Section 4 provides the simulation results. Section 5 concludes this paper.

2. Problem Formulation and Preliminaries

Problem Formulation

The n -link flexible-joint (FJ) robotic manipulator dynamics can be expressed as follows:

$$\begin{aligned} M\ddot{q}_1 + C(q_1, \dot{q}_1)\dot{q}_1 + G(q_1) + K(q_1 - q_2) &= d(t), \\ J\ddot{q}_2 + B\dot{q}_2 - K(q_1 - q_2) &= u(t) \end{aligned} \tag{1}$$

where $q_1, \dot{q}_1, \ddot{q}_1 \in R^n$ denote the link position, velocity, and acceleration vectors, respectively; $M(q) \in R^{n \times n}$ is the inertia matrix; $C(q, \dot{q}) \in R^{n \times n}$ is the centrifugal and Coriolis force matrix; $G(q) \in R^n$ is the gravity vector, $d(t)$ is the unknown disturbance vector; and $q_2, \dot{q}_2, \ddot{q}_2 \in R^n$ denote the rotor angular position, velocity, and acceleration vectors, respectively. The positive definite diagonal matrices $K \in R^{n \times n}$, $J \in R^{n \times n}$, and $B \in R^{n \times n}$ reflect the joint flexibility, actuator inertia, and natural damping term, respectively, and $u(t) \in R^n$ is the torque input. Here, we assume that $\lim_{t \rightarrow \infty} \dot{d}(t) = 0$.

Let $x_1 = [q_{11}, q_{12}, \dots, q_{1n}]^T$, $x_2 = \dot{x}_1 = [\dot{q}_{11}, \dot{q}_{12}, \dots, \dot{q}_{1n}]^T$, $x_3 = [q_{21}, q_{22}, \dots, q_{2n}]^T$ and $x_4 = \dot{x}_3 = [\dot{q}_{21}, \dot{q}_{22}, \dots, \dot{q}_{2n}]^T$. The dynamics of (1) then can be rewritten into the following form:

$$\begin{cases} \dot{x}_1 = x_2 \\ \dot{x}_2 = M^{-1}(-C(x_1, x_2)x_2 - G(x_1) - K(x_1 - x_3) + d(t)) \\ \dot{x}_3 = x_4 \\ \dot{x}_4 = J^{-1}(-Bx_4 + K(x_1 - x_3) + u(t)). \end{cases} \tag{2}$$

The control purpose of this paper is to design an NDO-based tracking controller to realize the following objectives: (i) The desired trajectory $x_d = [x_{d1}, x_{d2}, \dots, x_{dn}]^T$ can be tracked in the sense that $|z_{1i}(t)| = |x_{1i}(t) - x_{di}(t)| \leq \varepsilon$ as $t \rightarrow \infty$ where $\varepsilon > 0$ is a given precision, and all signals are guaranteed to be bounded. (ii) All states are required to be maintained in the following constraints

$$\begin{aligned} x_{di}(t) - F_{11}(t) < x_{1i}(t) < x_{di}(t) + F_{12}(t), \\ -F_{j1}(t) < x_{ji}(t) < F_{j2}(t) \end{aligned} \tag{3}$$

where $F_{ij}(t)$ are the prescribed constraints, with $i = 1, 2, \dots, n$, $j = 2, 3, 4$ being the positive time-varying functions, and their first and second derivatives are also continuous and bounded.

An NDO developed in [36] is used in this research to estimate the external unknown bounded continuous disturbance. For the sake of description, we describe the above system (2) into the following compact form:

$$\begin{aligned} \dot{x} &= f(x) + g_1(x)u + g_2(x)d, \\ y &= x_1 \end{aligned} \tag{4}$$

where $x = [x_1, x_2, x_3, x_4]^T$, and

$$f(x) = \begin{bmatrix} x_2 \\ M^{-1}(-C(x_1, x_2)x_2 - G(x_1) - K(x_1 - x_3)) \\ x_4 \\ J^{-1}(-Bx_4 + K(x_1 - x_3)) \end{bmatrix}$$

$$g_1(x) = \begin{bmatrix} 0_{n \times n} \\ 0_{n \times n} \\ 0_{n \times n} \\ J^{-1} \end{bmatrix}, g_2(x) = \begin{bmatrix} 0_{n \times n} \\ M^{-1} \\ 0_{n \times n} \\ 0_{n \times n} \end{bmatrix}.$$

The following NDO [36] is then employed to provide an online estimation of the disturbance $d(t)$:

$$\begin{cases} \dot{z} = -l(x)g_2(x)z - l(x)[g_2(x)p(x) + f(x) + g_1(x)u] \\ \hat{d} = z + p(x) \end{cases} \quad (5)$$

where l is the the gain matrix to be chosen. In this paper, the gain matrix l and p are chosen as $l(x) = [0_{n \times n}, M_{n \times n}, 0_{n \times n}, 0_{n \times n}]$ and $p(x) = [0_{n \times n}, M_{n \times n}x_2, 0_{n \times n}, 0_{n \times n}]$ to satisfy that

$$l(x)g_2(x) = \begin{pmatrix} 1 & \dots & 0 \\ \vdots & \ddots & \vdots \\ 0 & \dots & 1 \end{pmatrix}_{n \times n}.$$

Now, we define error $e = d(t) - \hat{d}(t)$, then it can be shown that $\dot{e} = -lg_2e + \dot{d}$, which implies that $\lim_{t \rightarrow \infty} e(t) = 0$ under the condition $\lim_{t \rightarrow \infty} \dot{d}(t) = 0$.

3. Controller Design and Stability Analysis

The control design procedure in this section can be summarized as follows: First, the constrained system under consideration is transformed into an unconstrained system using the SDF transformation. Subsequently, the tracking controller is designed using backstepping and filter technique to guarantee that the system states of the resulting closed-loop system are all bounded and do not exceed the constraint boundaries. In addition, we can make z_{1i} arbitrarily small by adjusting the design parameters. The control flow is shown in Figure 1.

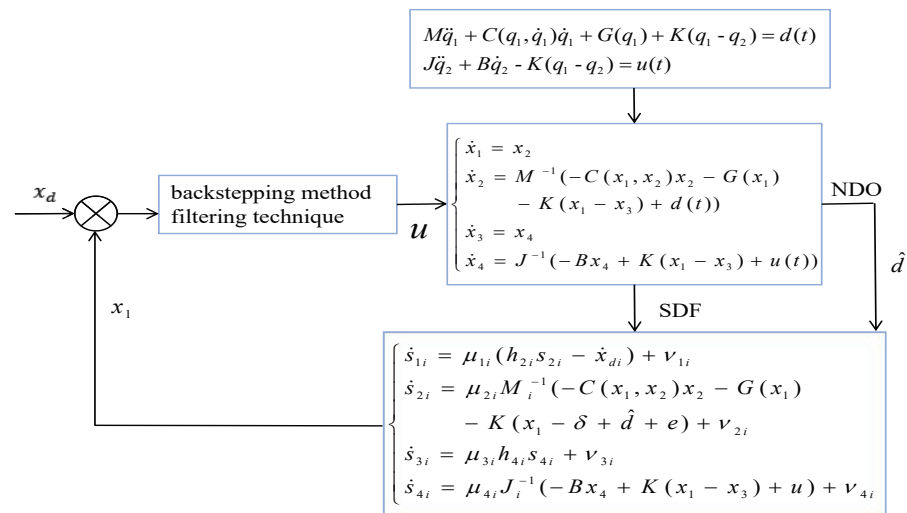


Figure 1. The control flow.

3.1. System Transformation

The SDF transformation is introduced to convert the original constrained system (4) into a new unconstrained system. After creating the tracking errors $z_{1i} = x_{1i} - x_{di}$, the subsequent functions can be introduced as [41]:

$$s_{1i} = \frac{z_{1i}}{(F_{11} + z_{1i})(F_{12} - z_{1i})}, s_{ji} = \frac{x_{ji}}{(F_{j1} + x_{ji})(F_{j2} - x_{ji})} \quad (6)$$

where $i = 1, 2, \dots, n, j = 2, 3, 4$. By introducing (6), the initial system (4) is changed into the new system described below:

$$\begin{cases} \dot{s}_{1i} = \mu_{1i}(h_{2i}s_{2i} - \dot{x}_{di}) + v_{1i} \\ \dot{s}_{2i} = \mu_{2i}M_i^{-1}(-C(x_1, x_2)x_2 - G(x_1) - K(x_1 - \delta + \hat{d} + e) + v_{2i} \\ \dot{s}_{3i} = \mu_{3i}h_{4i}s_{4i} + v_{3i} \\ \dot{s}_{4i} = \mu_{4i}J_i^{-1}(-Bx_4 + K(x_1 - x_3) + u) + v_{4i} \end{cases} \quad (7)$$

where

$$\begin{aligned} \mu_{1i} &= \frac{F_{11}F_{12} + z_{1i}^2}{(F_{11} + z_{1i})^2(F_{12} - z_{1i})^2}, \\ v_{1i} &= -\frac{[\dot{F}_{11}F_{12} + F_{11}\dot{F}_{12} + (\dot{F}_{12} - \dot{F}_{11})z_{1i}]z_{1i}}{(F_{11} + z_{1i})^2(F_{12} - z_{1i})^2}, \\ \mu_{ji} &= \frac{F_{j1}F_{j2} + x_{ji}^2}{(F_{j1} + x_{ji})^2(F_{j2} - x_{ji})^2}, \\ v_{ji} &= -\frac{[\dot{F}_{j1}F_{j2} + F_{j1}\dot{F}_{j2} + (\dot{F}_{j2} - \dot{F}_{j1})x_{ji}]x_{ji}}{(F_{j1} + x_{ji})^2(F_{j2} - x_{ji})^2}, \\ h_{1i} &= (F_{11} + z_{1i})(F_{12} - z_{1i}), \\ h_{ji} &= (F_{j1} + x_{ji})(F_{j2} - x_{ji}), \end{aligned}$$

$\delta = [h_{31}s_{31}, h_{32}s_{32}, \dots, h_{3n}s_{3n}]^T$ and $i = 1, 2, \dots, n, j = 2, 3, 4$. The constraint of $z_{1i}(t)$ is automatically guaranteed for every initial condition meeting $x_{di}(0) - F_{11}(0) < x_{1i}(0) < x_{di}(0) + F_{12}(0)$ as long as s_{1i} is constrained for $t \in [0, +\infty)$. It is crucial to guarantee the boundedness of s_{1i} for any $t > 0$ in order to satisfy the pre-specified constraint bound. If $\lim_{t \rightarrow \infty} s_{1i}(t) = 0$, then the asymptotic tracking control can be achieved.

Next, let us define $\beta(t) = H \tanh(\frac{1+\lambda t}{H})$, which is called a scaling function with $H > 1$ and $\lambda > 0$. The following characteristics of $\beta(t)$ are crucial for the subsequent work: (1) $\beta(t)$ strictly increases and $\beta(t) \geq \frac{1}{2}$ for all t ; (2) $\dot{\beta}(t) \leq \lambda\beta(t)$; and (3) $\lim_{t \rightarrow \infty} \beta(t) = H$.

Remark 1. The following characteristics of $s(x)$ are noteworthy: (i) $F_{11}(t)$ and $F_{12}(t)$ are smooth, time-varying, strictly positive functions. As a result, $s_{1i}(x)$ is invertible and strictly growing. (ii) $s_{1i}(0) = 0, s_{1i}(x) \rightarrow \infty$ as $x_{1i}(t) \rightarrow -F_{11}(t)$ or $x_{1i}(t) \rightarrow F_{12}(t)$.

3.2. Controller Design

To facilitate the controller design using the backstepping method, the following state transformations are given as:

$$w_{1i} = s_{1i}, w_{ji} = s_{ji} - \gamma_{ji} \quad (8)$$

in which $i = 1, 2, \dots, n, j = 2, 3, 4$ and γ_{ji} is the output of the first-order filter which is described as

$$\omega_{ji}\dot{\gamma}_{ji} = [\beta(\frac{\alpha_{j-1,i}}{h_{ji}} - \gamma_{ji})]^3 \quad (9)$$

where h_{ji} has been given above, $\alpha_{j-1,i}$ is the virtual control input and $\omega_{ji} > 0$ is a design parameter.

Then, in order to further achieve the aforementioned practical tracking control target, an error transformation is achieved by using the scaling function:

$$\zeta_{1i} = \beta w_{1i}, \zeta_{ji} = \beta w_{ji}. \quad (10)$$

In addition, we define

$$y_{ji} = \gamma_{ji} - \frac{\alpha_{j-1,i}}{h_{ij}}, Y_{ji} = \beta y_{ji} \tag{11}$$

which can ensure the stability of the first-order filter for subsequent stability analysis.

To achieve the desired control objective, we present the controller design step by step as follows:

Step 1: In this step, we choose a Lyapunov function as

$$V_1 = \sum_{i=1}^n V_{1i}, V_{1i} = \frac{1}{2} \zeta_{1i}^2 + \frac{1}{2} Y_{2i}^2. \tag{12}$$

Differentiating V_{1i} , one obtains

$$\dot{V}_{1i} = \zeta_{1i} \dot{\zeta}_{1i} + Y_{2i} \dot{Y}_{2i} \tag{13}$$

in which

$$\zeta_{1i} \dot{\zeta}_{1i} = \beta \zeta_{1i} (\mu_{1i} h_{2i} w_{2i} + \mu_{i1} h_{2i} y_{2i} - \mu_{1i} \dot{x}_{di} + v_{1i} + \beta^{-1} \dot{\beta} w_{1i}) + \beta \zeta_{1i} \mu_{1i} \alpha_{1i}, \tag{14}$$

and

$$\begin{aligned} Y_{2i} \dot{Y}_{2i} &\leq Y_{2i} (\beta \dot{y}_{2i} + \lambda \beta y_{2i}) \\ &= Y_{2i} [\beta (\dot{\gamma}_{2i} - (\frac{\alpha_{1i}}{h_{2i}})') + \lambda \beta y_{2i}] \\ &= -\frac{\beta Y_{2i}^4}{\omega_{2i}} + \beta \tilde{\zeta}_{2i} Y_{2i} + \lambda Y_{2i}^2 \end{aligned} \tag{15}$$

where $\tilde{\zeta}_{2i} = -\frac{\dot{\alpha}_{1i}}{h_{2i}} + \frac{\alpha_{1i} \dot{h}_{2i}}{h_{2i}^2}$.

Combining (13) with (14) and (15) yields that

$$\begin{aligned} \dot{V}_{1i} &\leq \beta \zeta_{1i} (\mu_{1i} h_{2i} w_{2i} + \mu_{i1} h_{2i} y_{2i} - \mu_{1i} \dot{x}_{di} \\ &\quad + v_{1i} + \beta^{-1} \dot{\beta} w_{1i}) + \beta \zeta_{1i} \mu_{1i} \alpha_{1i} - \frac{\beta Y_{2i}^4}{\omega_{2i}} + \beta \tilde{\zeta}_{2i} Y_{2i} + \lambda Y_{2i}^2. \end{aligned} \tag{16}$$

Using Young's inequality to calculate the terms on the right hand of (16), the following inequalities are obtained as:

$$\begin{aligned} \beta \zeta_{1i} \mu_{1i} h_{2i} w_{2i} &\leq \beta \mu_{1i}^2 \zeta_{1i}^2 h_{2i}^2 w_{2i}^2 + \frac{\beta}{4}, \\ \beta \zeta_{1i} \mu_{1i} h_{2i} y_{2i} &\leq \beta r_{1i} \zeta_{1i}^2 \mu_{1i}^2 + \frac{\beta}{4 r_{1i}} h_{2i}^2 Y_{2i}^2 \\ &\leq 2 r_{1i} \beta \zeta_{1i}^2 \mu_{1i}^2 + \frac{\beta}{2 r_{1i}} h_{2i}^4 Y_{2i}^4 + \frac{\beta}{8 r_{1i}}, \\ -\beta \zeta_{1i} \mu_{1i} \dot{x}_{di} &\leq r_{1i} \beta \mu_{1i}^2 \zeta_{1i}^2 \dot{x}_{di}^2 + \frac{\beta}{4 r_{1i}}, \\ \beta \zeta_{1i} v_{1i} &\leq \beta v_{1i} |\zeta_{1i}| \leq l_{1i} \beta \zeta_{1i}^2 v_{1i}^2 + \frac{\beta}{4 l_{1i}}, \\ \beta \zeta_{1i} \beta^{-1} \dot{\beta} w_{1i} &\leq l_{1i} \beta \lambda^2 \zeta_{1i}^2 w_{1i}^2 + \frac{\beta}{4 l_{1i}}, \\ \beta \tilde{\zeta}_{2i} Y_{2i} &\leq \frac{\beta \tilde{\zeta}_{2i}^2}{2} + \frac{\beta Y_{2i}^4}{4} + \frac{\beta}{4}, \\ \lambda Y_{2i}^2 &\leq \lambda^2 Y_{2i}^4 + \frac{1}{4}. \end{aligned}$$

Next, after a straightforward substitution, (16) can be rewritten as

$$\begin{aligned} \dot{V}_{1i} \leq & \beta\zeta_{1i}(\mu_{1i}\alpha_{1i} + r_{1i}\Phi_{1i}\zeta_{1i} + l_{1i}\Psi_{1i}\zeta_{1i}) + \beta\Delta_{1i} \\ & + \beta\zeta_{1i}^2\mu_{1i}^2h_{2i}^2w_{2i}^2 + \frac{\beta}{2r_{1i}}h_{2i}^4Y_{2i}^4 - \frac{\beta Y_{2i}^4}{\omega_{2i}} + \frac{\beta Y_{2i}^4}{4} + \frac{\beta\zeta_{2i}^2}{2} + \frac{\beta}{4} + \lambda^2Y_{2i}^4 + \frac{1}{4} \end{aligned} \quad (17)$$

in which $\Phi_{1i} = \mu_{1i}^2(x_{di}^2 + 2)$, $\Psi_{1i} = v_{1i}^2 + \lambda^2w_{1i}^2$ and $\Delta_{1i} = \frac{1}{4r_{1i}} + \frac{1}{8r_{1i}} + \frac{1}{2l_{1i}} + \frac{1}{4}$. In view of the structure of (17), the virtual controller is chosen as $\alpha_1 = A_1$ with

$$\begin{aligned} A_1 &= [A_{11}, A_{12}, \dots, A_{1n}]^T, \\ A_{1i} &= -\frac{1}{\mu_{1i}}(k_{1i} + r_{1i}\Phi_{1i} + l_{1i}\Psi_{1i})\zeta_{1i}. \end{aligned} \quad (18)$$

By selecting $\frac{1}{\omega_{2i}} \geq \frac{h_{2i}^4}{2r_{1i}} + \frac{1}{4} + \frac{\lambda^2}{\beta} + \omega_{2i}^*$ which represents a positive design parameter, and combining (17) and (18), we have

$$\dot{V}_{1i} \leq -k_{1i}\beta\zeta_{1i}^2 - \beta\omega_{2i}^*Y_{2i}^4 + \beta\varphi_{1i} + \beta\mu_{1i}^2\zeta_{1i}^2h_{2i}^2w_{2i}^2 + \frac{\beta\zeta_{2i}^2}{2} \quad (19)$$

where $\varphi_{1i} = \Delta_{1i} + \frac{3}{4}$, which further leads to

$$\dot{V}_1 \leq -\sum_{i=1}^n k_{1i}\beta\zeta_{1i}^2 - \sum_{i=1}^n \beta\omega_{2i}^*Y_{2i}^4 + \sum_{i=1}^n \beta\varphi_{1i} + \sum_{i=1}^n \beta\mu_{1i}^2\zeta_{1i}^2h_{2i}^2w_{2i}^2 + \sum_{i=1}^n \frac{\beta\zeta_{2i}^2}{2} \quad (20)$$

where the item $\sum_{i=1}^n \beta\mu_{1i}^2\zeta_{1i}^2h_{2i}^2w_{2i}^2$ will be dealt with in the following stage.

Step 2: The second candidate Lyapunov function is picked as

$$V_2 = \sum_{i=1}^n V_{2i}, V_{2i} = \frac{1}{2}\zeta_{2i}^2 + \frac{1}{2}Y_{3i}^2. \quad (21)$$

Then, it is simple to derive the time derivative of V_{2i} as

$$\begin{aligned} \dot{V}_{2i} &= \zeta_{2i}\dot{\zeta}_{2i} + Y_{3i}\dot{Y}_{3i} \\ &\leq \beta\zeta_{2i}(\mu_{2i}\Gamma_{1i} + \mu_{2i}M_i^{-1}(K\tau + K\sigma + e) + v_{2i} - \dot{\gamma}_{2i} + \beta^{-1}\dot{\beta}w_{2i}) \\ &\quad + \beta\zeta_{2i}\mu_{2i}M_i^{-1}K\alpha_2 - \frac{\beta Y_{3i}^4}{\omega_{3i}} + \beta\zeta_{3i}Y_{3i} + \lambda Y_{3i}^2 \end{aligned} \quad (22)$$

where $\Gamma_{1i} = M_i^{-1}(-C(x_1, x_2)x_2 - G(x_1) - Kx_1 + \hat{d})$, $\zeta_{3i} = -\frac{\dot{\alpha}_{2i}}{h_{3i}} + \frac{\alpha_{2i}h_{3i}}{h_{3i}^2}$, $\tau = [h_{31}w_{31}, h_{32}w_{32}, \dots, h_{3n}w_{3n}]^T$, $\sigma = [h_{31}y_{31}, h_{32}y_{32}, \dots, h_{3n}y_{3n}]^T$. Then, using Young's inequality, one has

$$\begin{aligned}
 \beta\zeta_{2i}\mu_{2i}\Gamma_{1i} &\leq r_{2i}\beta\zeta_{2i}^2\mu_{2i}^2\Gamma_{1i}^2 + \frac{\beta}{4r_{2i}}, \\
 \beta\zeta_{2i}\mu_{2i}\Lambda_{1i}\tau &\leq \beta\zeta_{2i}^2\mu_{2i}^2\tau^T\tau + \frac{\beta}{4}\Lambda_{1i}\Lambda_{1i}^T, \\
 \beta\zeta_{2i}\mu_{2i}\Lambda_{1i}\sigma &\leq 2\beta r_{2i}\zeta_{2i}^2\mu_{2i}^2 + \frac{\beta}{2r_{2i}}\rho^T\rho + \frac{\beta}{8r_{2i}}(\Lambda_{1i}\Lambda_{1i}^T)^2, \\
 \beta\zeta_{2i}\mu_{2i}M_i^{-1}e &\leq r_{2i}\beta\zeta_{2i}^2\mu_{2i}^2 + \frac{\beta}{4r_{2i}}\|M_i^{-1}\|^2 e^T e, \\
 \beta\zeta_{2i}v_{2i} &\leq l_{2i}\beta\zeta_{2i}^2v_{2i}^2 + \frac{\beta}{4l_{2i}}, \\
 -\beta\zeta_{2i}\dot{\gamma}_{2i} &\leq l_{2i}\beta\zeta_{2i}^2\dot{\gamma}_{2i}^2 + \frac{\beta}{4l_{2i}}, \\
 \beta\zeta_{2i}\beta^{-1}\dot{\beta}w_{2i} &\leq l_{2i}\beta\lambda^2\zeta_{2i}^2w_{2i}^2 + \frac{\beta}{4l_{2i}}, \\
 \beta\zeta_{3i}Y_{3i} &\leq \frac{\beta\zeta_{3i}^2}{2} + \frac{\beta Y_{3i}^2}{4} + \frac{\beta}{4}
 \end{aligned}$$

and

$$\lambda Y_{3i}^2 \leq \lambda^2 Y_{3i}^2 + \frac{1}{4}$$

where $\Lambda_{1i} = M_i^{-1}K$, $\rho = [h_{31}Y_{31}, h_{32}Y_{32}, \dots, h_{3n}Y_{3n}]^T$. As a result, we can obtain the following result as

$$\begin{aligned}
 \dot{V}_{2i} &\leq \beta\zeta_{2i}(\mu_{2i}\Lambda_{1i}\alpha_2 + r_{2i}\Phi_{2i}\zeta_{2i} + l_{2i}\Psi_{2i}\zeta_{2i}) + \beta\Delta_{2i} + \beta\zeta_{2i}^2\mu_{2i}^2\tau^T\tau \\
 &\quad + \frac{\beta}{4r_{2i}}\|M_i^{-1}\|^2 e^T e + \frac{\beta}{2r_{2i}}\rho^T\rho - \frac{\beta Y_{3i}^4}{\omega_{3i}} + \frac{\beta Y_{3i}^4}{4} + \frac{\beta\zeta_{3i}^2}{2} + \frac{\beta}{4} + \lambda^2 Y_{3i}^4 + \frac{1}{4} \quad (23)
 \end{aligned}$$

where $\Delta_{2i} = \frac{1}{4r_{2i}} + \frac{1}{4}\Lambda_{1i}\Lambda_{1i}^T + \frac{1}{8r_{2i}}(\Lambda_{1i}\Lambda_{1i}^T)^2 + \frac{3}{4l_{2i}}$, $\Phi_{2i} = 3\mu_{2i}^2 + \Gamma_{1i}^2\mu_{2i}^2$ and $\Psi_{2i} = v_{2i}^2 + \dot{\gamma}_{2i}^2 + \lambda^2 w_{2i}^2$.

The virtual controller in (23) is chosen as

$$\alpha_2 = K^{-1}MA_2 \quad (24)$$

where $A_2 = [A_{21}, A_{22}, \dots, A_{2n}]^T$, and a detailed description of A_{2i} is given as

$$A_{2i} = -\frac{1}{\mu_{2i}}(k_{2i} + r_{2i}\Phi_{2i} + l_{2i}\Psi_{2i} + \mu_{1i}^2w_{1i}^2h_{2i}^2)\zeta_{2i} - \beta\mu_{2i}\zeta_{2i}\tau^T\tau. \quad (25)$$

Then, by selecting $\frac{1}{\omega_{3i}} \geq \frac{1}{4} + \frac{\lambda^2}{\beta} + \omega_{3i}^*$, (23) can be rewritten as

$$\begin{aligned}
 \dot{V}_{2i} &\leq -k_{2i}\beta\zeta_{2i}^2 - \beta\omega_{3i}^*Y_{3i}^4 + \beta\varphi_{2i} - \beta\mu_{1i}^2\zeta_{1i}^2h_{2i}^2w_{2i}^2 \\
 &\quad + \frac{\beta}{4r_{2i}}\|M_i^{-1}\|^2 e^T e + \frac{\beta}{2r_{2i}}\rho^T\rho + \frac{\beta\zeta_{3i}^2}{2} \quad (26)
 \end{aligned}$$

where $\varphi_{2i} = \Delta_{2i} + \frac{3}{4}$. This ultimately results in

$$\begin{aligned}
 \dot{V}_2 &\leq -\sum_{i=1}^n k_{2i}\beta\zeta_{2i}^2 - \sum_{i=1}^n \beta\omega_{3i}^*Y_{3i}^4 + \sum_{i=1}^n \beta\varphi_{2i} + \sum_{i=1}^n \beta\mu_{1i}^2\zeta_{1i}^2h_{2i}^2w_{2i}^2 \\
 &\quad + \sum_{i=1}^n \frac{\beta\zeta_{3i}^2}{2} + \sum_{i=1}^n \frac{\beta}{4r_{2i}}\|M_i^{-1}\|^2 e^T e + \sum_{i=1}^n \frac{\beta}{2r_{2i}}\rho^T\rho. \quad (27)
 \end{aligned}$$

Step 3: The candidate Lyapunov function is defined as:

$$V_3 = \sum_{i=1}^n V_{3i}, V_{3i} = \frac{1}{2}\zeta_{3i}^2 + \frac{1}{2}Y_{4i}^2. \tag{28}$$

The time derivative of V_{3i} is computed as

$$\begin{aligned} \dot{V}_{3i} &= \zeta_{3i}\dot{\zeta}_{3i} + Y_{4i}\dot{Y}_{4i} \\ &\leq \beta\zeta_{2i}(\mu_{3i}h_{4i}w_{4i} + \mu_{3i}h_{4i}y_{4i} + v_{3i} - \dot{\gamma}_{3i} \\ &\quad + \beta^{-1}\dot{\beta}w_{3i}) + \beta\zeta_{3i}\mu_{3i}\alpha_{3i} - \frac{\beta Y_{4i}^4}{\omega_{4i}} + \beta\zeta_{4i}Y_{4i} + \lambda Y_{4i}^2 \end{aligned} \tag{29}$$

where $\zeta_{4i} = -\frac{\dot{\alpha}_{3i}}{h_{4i}} + \frac{\alpha_{3i}h_{4i}}{h_{4i}^2}$. Similar to Step 1 and Step 2, direct calculation produces

$$\begin{aligned} \dot{V}_{3i} &\leq \beta\zeta_{3i}(\mu_{3i}\alpha_{3i} + r_{3i}\Phi_{3i}\zeta_{3i} + l_{3i}\Psi_{3i}\zeta_{3i}) + \beta\Delta_{3i} + \beta\zeta_{3i}^2\mu_{3i}^2h_{4i}^2w_{4i}^2 \\ &\quad + \frac{\beta}{2r_{3i}}h_{4i}^4Y_{4i}^4 - \frac{\beta Y_{4i}^4}{\omega_{4i}} + \frac{\beta Y_{4i}^4}{4} + \frac{\beta\zeta_{4i}^2}{2} + \frac{\beta}{4} + \lambda^2Y_{4i}^4 + \frac{1}{4} \end{aligned} \tag{30}$$

where $\Phi_{3i} = 2\mu_{3i}^2$, $\Psi_{3i} = v_{3i}^2 + \dot{\gamma}_{3i}^2 + \lambda^2w_{3i}^2$ and $\Delta_{3i} = \frac{1}{8r_{3i}} + \frac{3}{4r_{3i}} + \frac{1}{4}$.

The third virtual control law α_3 can be written as $\alpha_3 = A_3$ with

$$\begin{aligned} A_3 &= [A_{31}, A_{32}, \dots, A_{3n}]^T, \\ A_{3i} &= -\frac{1}{\mu_{3i}}(k_{3i} + r_{3i}\Phi_{3i} + l_{3i}\Psi_{3i})\zeta_{3i}. \end{aligned} \tag{31}$$

By choosing $\frac{1}{\omega_{4i}} \geq \frac{h_{4i}^4}{2r_{3i}} + \frac{1}{4} + \frac{\lambda^2}{\beta} + \omega_{4i}^*$, one can obtain

$$\dot{V}_{3i} \leq -k_{3i}\beta\zeta_{3i}^2 - \beta\omega_{4i}^*Y_{4i}^4 + \beta\varphi_{3i} + \frac{\beta\zeta_{4i}^2}{2} + \beta\mu_{3i}^2\zeta_{3i}^2h_{4i}^2w_{4i}^2 \tag{32}$$

where $\varphi_{3i} = \Delta_{3i} + \frac{3}{4}$. Under (30), the following result can be expressed as

$$\dot{V}_3 \leq -\sum_{i=1}^n k_{3i}\beta\zeta_{3i}^2 - \sum_{i=1}^n \beta\omega_{4i}^*Y_{4i}^4 + \sum_{i=1}^n \beta\varphi_{3i} + \sum_{i=1}^n \frac{\beta\zeta_{4i}^2}{2} + \sum_{i=1}^n \beta\mu_{3i}^2\zeta_{3i}^2h_{4i}^2w_{4i}^2. \tag{33}$$

Step 4: Taking into account the following Lyapunov function $V_4 = \sum_{i=1}^n V_{4i}$, $V_{4i} = \frac{1}{2}\zeta_{4i}^2$, it is simple to derive the time derivative of V_{4i} as

$$\begin{aligned} \dot{V}_{4i} &= \zeta_{4i}\dot{\zeta}_{4i} \\ &\leq \beta\zeta_{4i}(\mu_{4i}\Gamma_{2i} + v_{4i} - \dot{\gamma}_{4i} + \beta^{-1}\dot{\beta}w_{4i}) + \beta\zeta_{4i}\mu_{4i}J_i^{-1}u \end{aligned} \tag{34}$$

where $\Gamma_{2i} = J_i^{-1}(-Bx_4 + K(x_1 - x_3))$. Using Young's inequality and the analysis described in the previous steps, we have

$$\dot{V}_{4i} \leq \beta\zeta_{4i}(r_{4i}\Phi_{4i}\zeta_{4i} + l_{4i}\Psi_{4i}\zeta_{4i}) + \beta\Delta_{4i} + \beta\zeta_{4i}\mu_{4i}J_i^{-1}u \tag{35}$$

where $\Phi_{4i} = \mu_{4i}^2\Gamma_{2i}^2$, $\Psi_{4i} = v_{4i}^2 + \dot{\gamma}_{4i}^2 + \lambda^2w_{4i}^2$, and $\Delta_{4i} = \frac{1}{4r_{4i}} + \frac{3}{4r_{4i}}$.

In this final step, the actual control law u is configured as $u = JA_4$ where

$$\begin{aligned} A_4 &= [A_{41}, A_{42}, \dots, A_{4n}]^T, \\ A_{4i} &= -\frac{1}{\mu_{4i}}(k_{4i} + r_{4i}\Phi_{4i} + l_{4i}\Psi_{4i} + \mu_{3i}^2w_{3i}^2h_{4i}^2)\zeta_{4i}. \end{aligned} \tag{36}$$

Substituting u into (35), we obtain that

$$\dot{V}_{4i} \leq -k_{4i}\beta\zeta_{4i}^2 - \beta\mu_{3i}^2\zeta_{3i}^2h_{4i}^2w_{4i}^2 + \beta\varphi_{4i} \tag{37}$$

where $\varphi_{4i} = \Delta_{4i}$, which further leads to

$$\dot{V}_4 \leq -\sum_{i=1}^n k_{4i}\beta\zeta_{4i}^2 - \sum_{i=1}^n \beta\mu_{3i}^2\zeta_{3i}^2h_{4i}^2w_{4i}^2 + \sum_{i=1}^n \beta\varphi_{4i}. \tag{38}$$

Thus, the entire design process for the tracking controller is described in detail.

3.3. Stability Analysis

Using the previous analysis, the result of this section can be presented in the following theorem.

Theorem 1. *For the n -link FJ manipulator system formulated by (1), based on the introduced nonlinear disturbance observer (5), the tracking control law u defined by (36) can achieve the following objectives:*

- (i) *The states of the resulting closed-loop system are bounded and do not violate the constraints for all t .*
- (ii) *For any given $\varepsilon > 0$, there exist proper design parameters such that the tracking error $z_{1i}(t)$ satisfies $|z_{1i}(t)| \leq \varepsilon$ as $t \rightarrow \infty$, and the error signal $z_{1i}(t)$ can be made arbitrarily small.*

Proof. Combining Formulas (20), (27), (33), and (38), we can have

$$\begin{aligned} \dot{V} &= \dot{V}_1 + \dot{V}_2 + \dot{V}_3 + \dot{V}_4 \\ &\leq -\sum_{j=1}^4 \sum_{i=1}^n k_{ji}\beta\zeta_{ji}^2 - \sum_{j=2}^4 \sum_{i=1}^n \beta\omega_{ji}^*Y_{ji}^4 + \sum_{j=1}^4 \sum_{i=1}^n \beta\varphi_{ji} \\ &\quad + \sum_{j=2}^4 \sum_{i=1}^n \frac{\beta\zeta_{ji}^2}{2} + \sum_{i=1}^n \frac{\beta}{4r_{2i}} \|M_i^{-1}\|^2 e^T e + \sum_{i=1}^n \frac{\beta}{2r_{2i}} \rho^T \rho. \end{aligned} \tag{39}$$

Then, the following compact sets are defined as $\Omega_V = \{ \sum_{j=1}^4 \sum_{i=1}^n \zeta_{ji}^2 + \sum_{j=2}^4 \sum_{i=1}^n Y_{ji}^2 \leq 2\delta \} \subset \mathbb{R}^{8n-1}$, $\Omega_x = \{ [x_{di}, \dot{x}_{di}, \ddot{x}_{di}]^T : x_{di}^2 + \dot{x}_{di}^2 + \ddot{x}_{di}^2 \leq \gamma \} \subset \mathbb{R}^{3n}$ with δ and γ being the positive constants. In the compact set $\Omega_V \times \Omega_x$, there are positive constants θ_{ji} and \bar{h}_3 such that $|\zeta_{ji}| \leq \theta_{ji}$ and $h_{3i}^2 \leq \bar{h}_3$.

Thus, by using Young’s inequality, we have $y_i^2 \leq y_i^4 + \frac{1}{4}$. Now, (39) can be rewritten as

$$\begin{aligned} \dot{V} &\leq -\sum_{j=1}^4 \sum_{i=1}^n k_{ji}\beta\zeta_{ji}^2 - \sum_{j=2}^4 \sum_{i=1}^n \beta\omega_{ji}^*Y_{ji}^2 + \beta\sigma_1 + \beta\tau_1 \\ &\leq -\beta\eta_1 V + \beta\sigma_1 + \beta\tau_1 \end{aligned} \tag{40}$$

where ω_{3i}^* has been updated as $\omega_{3i}^* - \bar{h}_3 / (2r_{2i}) > 0$, $\eta_1 = \min \{ 2k_{ji}, 2\omega_{ji}^* \}$, $\sigma_1 = \sum_{j=1}^4 \sum_{i=1}^n \varphi_{ji} + \frac{1}{2} \sum_{j=1}^4 \sum_{i=1}^n \theta_{ji}^2 + \frac{1}{4} \sum_{j=2}^4 \sum_{i=1}^n \omega_{ji}^*$, $\tau_1 = \sum_{i=1}^n \frac{\beta}{4r_{2i}} e^T e \cdot \|M_i^{-1}\|^2$. By selecting $o = \frac{\sigma_1 + \tau_1}{\eta_1}$, as a result, we can obtain that $V = o$ for $\dot{V} = 0$. So, if $V(0) \leq o$, then $V(t) \leq o$ for $t \geq 0$. Then, by multiplying (40) by $e^{\eta_1 \int_0^t \beta(s) ds}$, one readily has

$$\frac{d}{dt} (e^{\eta_1 \int_0^t \beta(s) ds} V(t)) \leq e^{\eta_1 \int_0^t \beta(s) ds} \beta(\sigma_1 + \tau_1). \tag{41}$$

Integrating (41) from 0 to t yields that

$$\begin{aligned}
 V(t) &\leq e^{-\eta_1 \int_0^t \beta(s) ds} V(0) + \sigma_1 e^{-\eta_1 \int_0^t \beta(s) ds} \int_0^t e^{\eta_1 \int_0^q \beta(s) ds} \beta(q) dq \\
 &\quad + e^{-\eta_1 \int_0^t \beta(s) ds} \int_0^t e^{\eta_1 \int_0^q \beta(s) ds} \tau_1(q) \beta(q) dq.
 \end{aligned}
 \tag{42}$$

On the right-hand side of (42), we compute the second term to obtain

$$\begin{aligned}
 \sigma_1 e^{-\eta_1 \int_0^t \beta(s) ds} \int_0^t e^{\eta_1 \int_0^q \beta(s) ds} \beta(q) dq &= \sigma_1 e^{-\eta_1 \int_0^t \beta(s) ds} \int_0^t e^{\eta_1 \int_0^q \beta(s) ds} d\left(\int_0^q \beta(s) ds\right) \\
 &= \frac{\sigma_1}{\eta_1} e^{-\eta_1 \int_0^t \beta(s) ds} \left(e^{\eta_1 \int_0^q \beta(s) ds} \Big|_0^t \right) \leq \frac{\sigma_1}{\eta_1}.
 \end{aligned}
 \tag{43}$$

Since $\lim_{t \rightarrow \infty} \tau_1(t) = 0$, it can be deduced that there is a constant $c > 0$ such that $|\tau_1(t)| < \varepsilon$ as $t > c$. For the third term on the right-hand side of (42), we have

$$\begin{aligned}
 &e^{-\eta_1 \int_0^t \beta(s) ds} \int_0^t e^{\eta_1 \int_0^q \beta(s) ds} \tau_1(q) \beta(q) dq \\
 &= e^{-\eta_1 \int_0^t \beta(s) ds} \int_0^c e^{\eta_1 \int_0^q \beta(s) ds} \tau_1(q) \beta(q) dq \\
 &\quad + e^{-\eta_1 \int_0^t \beta(s) ds} \int_c^t e^{\eta_1 \int_c^q \beta(s) ds} \tau_1(q) \beta(q) dq.
 \end{aligned}
 \tag{44}$$

The term $e^{-\eta_1 \int_0^t \beta(s) ds} \int_0^c e^{\eta_1 \int_0^q \beta(s) ds} \tau_1(q) \beta(q) dq \rightarrow 0$ as $t \rightarrow \infty$, and the term $e^{-\eta_1 \int_0^t \beta(s) ds} \int_c^t e^{\eta_1 \int_c^q \beta(s) ds} \tau_1(q) \beta(q) dq$ satisfies

$$\begin{aligned}
 &e^{-\eta_1 \int_0^t \beta(s) ds} \int_c^t e^{\eta_1 \int_c^q \beta(s) ds} \tau_1(q) \beta(q) dq \\
 &\leq \varepsilon e^{-\eta_1 \int_0^t \beta(s) ds} \int_c^t e^{\eta_1 \int_c^q \beta(s) ds} \beta(q) dq \\
 &\leq \frac{\varepsilon}{\eta_1} e^{-\eta_1 \int_0^t \beta(s) ds} \left(e^{\eta_1 \int_c^q \beta(s) ds} \Big|_c^t \right) \leq \frac{\varepsilon}{\eta_1}.
 \end{aligned}
 \tag{45}$$

Finally, combining (44) and (45) yields that

$$\begin{aligned}
 V(t) &\leq e^{-\eta_1 \int_0^t \beta(s) ds} V(0) + \frac{\sigma_1}{\eta_1} + \frac{\varepsilon}{\eta_1} \\
 &\leq V(0) + \frac{\sigma_1}{\eta_1} + \frac{\varepsilon}{\eta_1}.
 \end{aligned}
 \tag{46}$$

For any initial condition $x_{ji}(0)$ satisfying the desired constraints, in view of (46), we have $V \in L_\infty$, so $\zeta_{ji} \in L_\infty$, $Y_{ji} \in L_\infty$. Considering (10) and (11), one can get $w_{ji} = \beta^{-1} \zeta_{ji} \in L_\infty$, $y_{ji} = \beta^{-1} Y_{ji} \in L_\infty$. Further, it is easy to acquire that according to (7) and (8), x_{1i} is constrained since the desired trajectory x_{di} is constrained. Nevertheless, as $w_{ji} \in L_\infty$, it follows that if $-F_{11}(0) < z_{1i}(0) < F_{12}(0)$, then $-F_{11}(t) < z_{1i}(t) < F_{12}(t)$. When the inequality $(F_{11}(t) + z_{1i}(t))(F_{12}(t) - z_{1i}(t)) < (F_{11}(t) + F_{12}(t))^2$ is applied, one has $|z_{1i}(t)| \leq \frac{F}{H} \sqrt{2(V(0) + \frac{\sigma_1}{\eta_1} + \frac{\varepsilon}{\eta_1})}$ as $t \rightarrow \infty$, where $F = \max_{t \geq 0} (F_{11}(t) + F_{12}(t))^2$. Thus, $\forall \varepsilon > 0$, one chooses $H > \frac{F}{\varepsilon} \sqrt{2(V(0) + \frac{\sigma_1}{\eta_1} + \frac{\varepsilon}{\eta_1})}$ to ensure that the practical tracking is realized since the tracking error $z_{1i}(t)$ satisfies $|z_{1i}(t)| \leq \varepsilon$ as $t \rightarrow \infty$.

Now, it is easy to conclude that $\gamma_{ji} \in L_\infty$, $s_{1i} \in L_\infty$, $s_{ji} \in L_\infty$ with $(j = 2, 3, 4)$, which further suggests that $\alpha_{j-1,i}$, u are bounded. As a result, all signals of the resulting closed-loop system are bounded and remain within the time-varying constrained regions for all time. The proof is now complete. \square

Remark 2. Different from the BLF method, which is commonly used to solve the constraint problem such as [33], this paper adopts the SDF-based control method, which does not need to consider the influence of the feasibility conditions on the virtual controller, and simplifies the control design. Compared with the single-link FJ manipulator in [35,40], the studied system in this paper belongs to a class of complex MIMO systems, which means that the proposed control method has a wider application range. In addition, we considered the presence of the mismatched disturbance.

Remark 3. In this paper, the control design of the DO-based tracking controller relies on the known system parameters $M, C, G, B,$ and $K,$ which is one of the limitations of the proposed approach. On the other hand, the backlash and flexibility are not considered temporarily in this paper. Therefore, our future works will focus on the compensation problem of the backlash and hysteresis for uncertain FJ manipulators such as [42].

4. Simulation Results

In this section, a two-link FJ manipulator system is used as an example to verify the feasibility of the proposed tracking controller based on the introduced NDO (5), whose dynamic equation is expressed as

$$\begin{aligned} M\ddot{q}_1 + C(q_1, \dot{q}_1)\dot{q}_1 + G(q_1) + K(q_1 - q_2) &= d(t), \\ J\ddot{q}_2 + B\dot{q}_2 - K(q_1 - q_2) &= u(t) \end{aligned} \tag{47}$$

where $x_1 = [x_{11}, x_{12}]^T = q_1 = [q_{11}, q_{12}]^T, x_2 = [x_{21}, x_{22}]^T = \dot{q}_1 = [\dot{q}_{11}, \dot{q}_{12}]^T, x_3 = [x_{31}, x_{32}]^T = q_2 = [q_{21}, q_{22}]^T, x_4 = [x_{41}, x_{42}]^T = \dot{q}_2 = [\dot{q}_{21}, \dot{q}_{22}]^T, B = \text{diag}[B_1, B_2], J = \text{diag}[J_1, J_2],$ and $K = \text{diag}[K_1, K_2].$ Combining system (2), we have $d = [d_1, d_2]^T, u = [u_1, u_2]^T.$ The detailed expressions of M, C and G can be founded in [43]. It should be noted that $M, C,$ and G can be calculated as long as some physical parameters of the FJ manipulator are known. In simulation, the parameters of the two-link FJ manipulator system are given in Table 1.

Table 1. Parameters of the two-link FJ manipulator system.

Variables/Parameters	Meaning	Value	Unit
m_1	mass of rod 1	1	kg
m_2	mass of rod 2	1	kg
l_1	length of rod 1	1	m
l_2	length of rod 2	1	m
J_1	joint flexibility of rod 1	1	m/s ²
J_2	joint flexibility of rod 2	1	m/s ²
B_1	damping factor of rod 1	0.1	none
B_2	damping factor of rod 2	0.1	none
K_1	joint stiffness of rod 1	100	N · m · /rad
K_2	joint stiffness of rod 2	100	N · m · /rad
g	gravitational acceleration	9.8	m/s ²

The external disturbances are selected as $d_1(t) = \frac{1}{1+t} + 1, d_2(t) = \frac{1}{1+t} + 1.$ The reference trajectories are defined as $x_{d1} = 0.5 \sin t, x_{d2} = 0.5 \sin t.$ Now, the control objectives can be described as (1) output variables x_{11}, x_{12} can track $x_{d1} = 0.5 \sin t, x_{d2} = 0.5 \sin t,$ and (2) the following full-state constraints are realized: $x_{d1}(t) - F_{11}(t) < x_{11}(t) < x_{d1}(t) + F_{12}(t), x_{d2}(t) - F_{11}(t) < x_{12}(t) < x_{d2}(t) + F_{12}(t), -F_{21}(t) < x_{21}(t) < F_{22}(t), -F_{21}(t) < x_{22}(t) < F_{22}(t), -F_{31}(t) < \dot{x}_{11}(t) < F_{32}(t), -F_{31}(t) < \dot{x}_{12}(t) < F_{32}(t), -F_{41}(t) < \dot{x}_{21}(t) < F_{42}(t), -F_{41}(t) < \dot{x}_{22}(t) < F_{42}(t),$ where $F_{11}(t) = F_{12}(t) = F_{21}(t) = F_{22}(t) = F_{31}(t) = F_{32}(t) = F_{41}(t) = F_{42}(t) = 5.$ The initial conditions are set as $x_1(0) = [0, 0]^T, x_2(0) = [0, 0]^T, x_3(0) = [0, 0]^T, x_4(0) = [0, 0]^T, \gamma_2(0) = [\gamma_{21}(0), \gamma_{22}(0)], \gamma_3(0) = [\gamma_{31}(0), \gamma_{32}(0)], \gamma_4(0) = [\gamma_{41}(0), \gamma_{42}(0)].$ The design parameters are chosen as $k_{11} = k_{12} = 2.5, k_{21} = k_{22} = 4.5, k_{31} = 0.1, k_{32} = 0.15, k_{41} = 5, k_{42} = 25, r_{11} = r_{12} = r_{21} = r_{22} = r_{31} = r_{32} = r_{41} = r_{42} = l_{11} = l_{12} = l_{21} = l_{22} = l_{31} = l_{32} = l_{41} = l_{42} = 0.001, \omega_{21} = \omega_{22} = 0.001, \omega_{31} = \omega_{32} = 0.0015, \omega_{41} = \omega_{42} = 0.0001, \lambda = 0.8.$

The simulation results are shown in Figures 2–7. From Figures 2 and 3, it can be seen that the outputs x_{11} and x_{12} of the two-link FJ manipulator can effectively track the reference

trajectories x_{d1} and x_{d2} , and all system states are within the constraint boundaries. As depicted in Figures 4 and 5, the virtual control signals and outputs of the first-order filter are bounded, which also indicate the reliability of the filter’s performance. Figure 6 shows that the disturbance estimation $\hat{d}(t)$ generated by the NDO can converge asymptotically to the true disturbances $d(t)$, which emphasizes the effectiveness of NDO. Figure 7 illustrates that the control inputs are also bounded. These results clearly demonstrate that the suggested approach effectively achieves the desirable control performance, successfully meeting the specified control objectives.

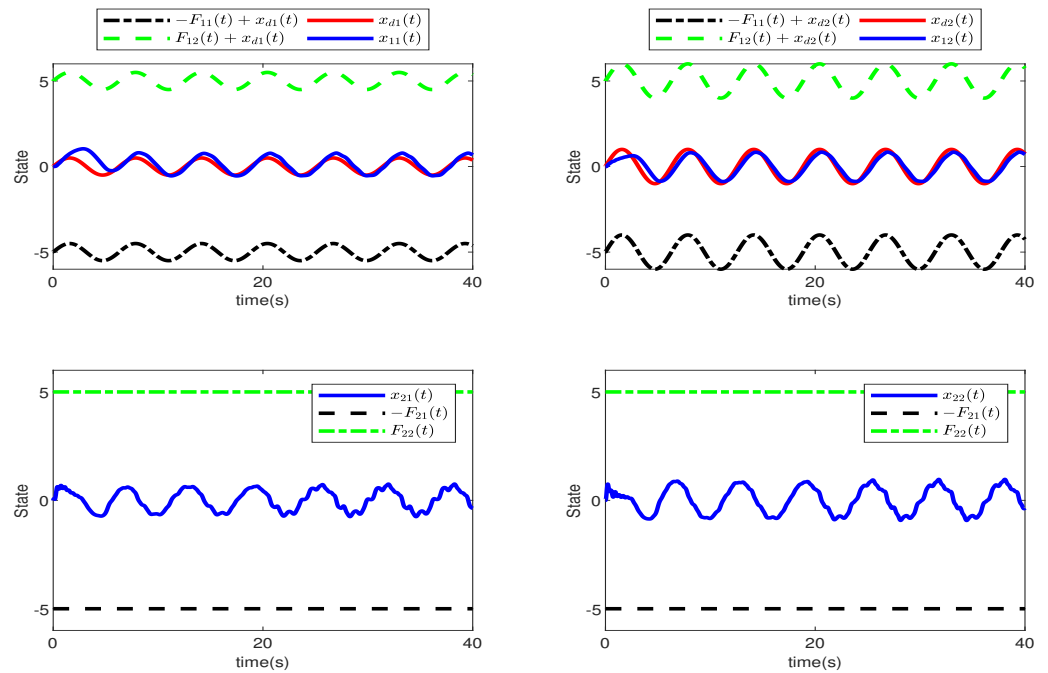


Figure 2. The responses of states x_{11} , x_{12} , x_{21} , and x_{22} .

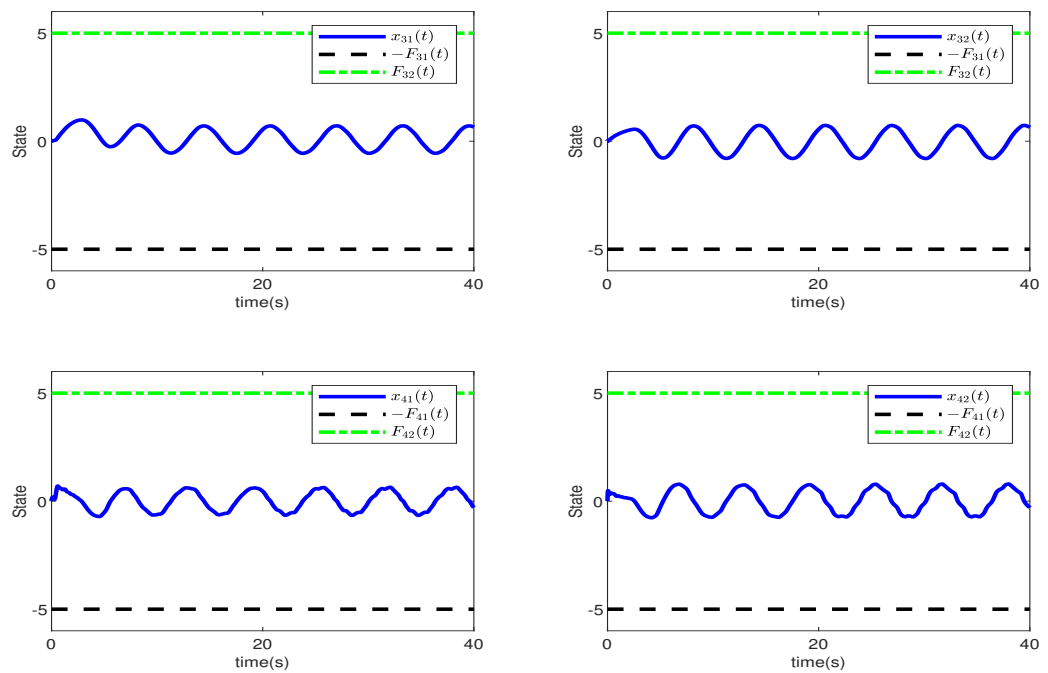


Figure 3. The responses of states x_{31} , x_{32} , x_{41} , and x_{42} .

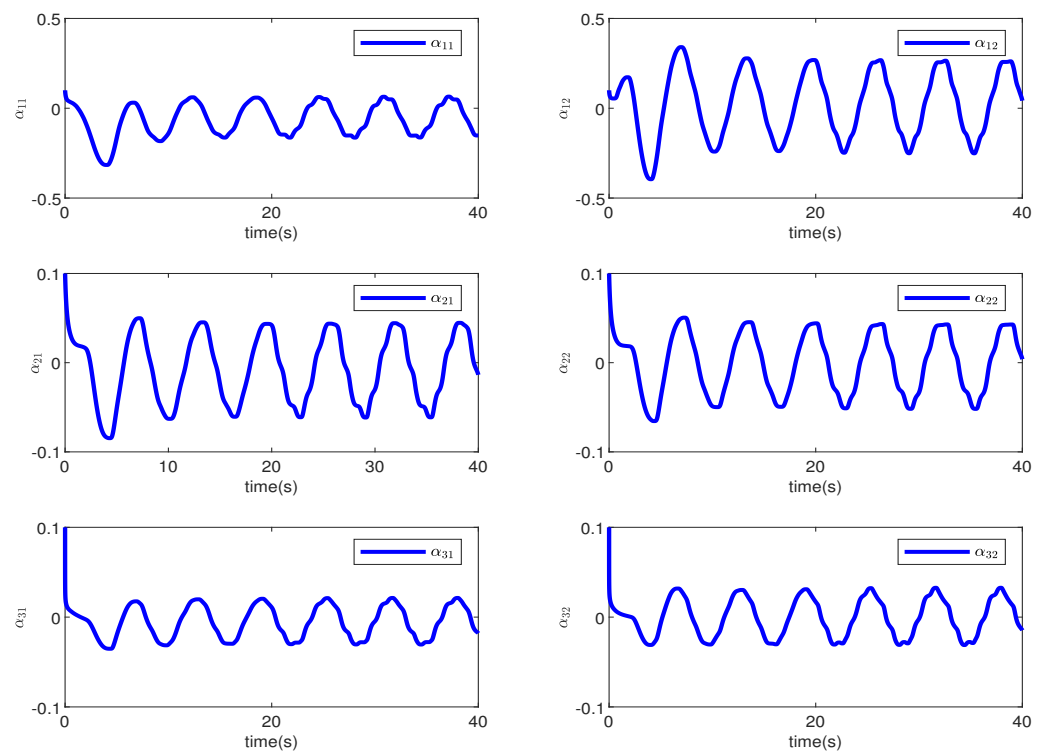


Figure 4. The responses of virtual control signals.

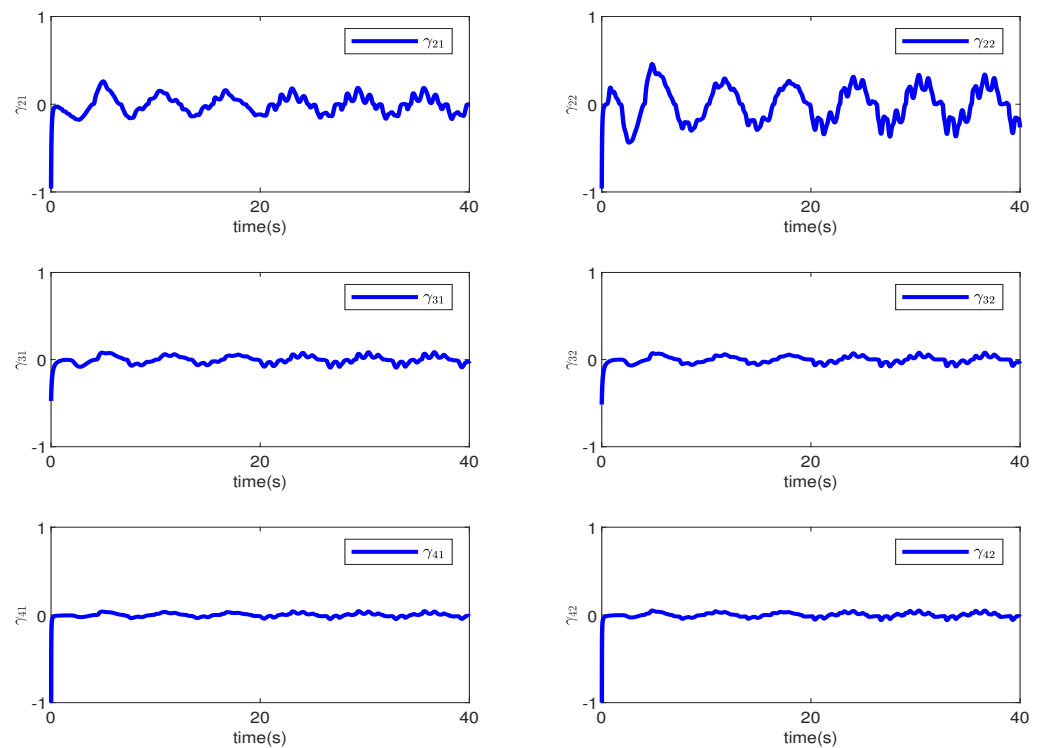


Figure 5. The responses of first-order filters' states.

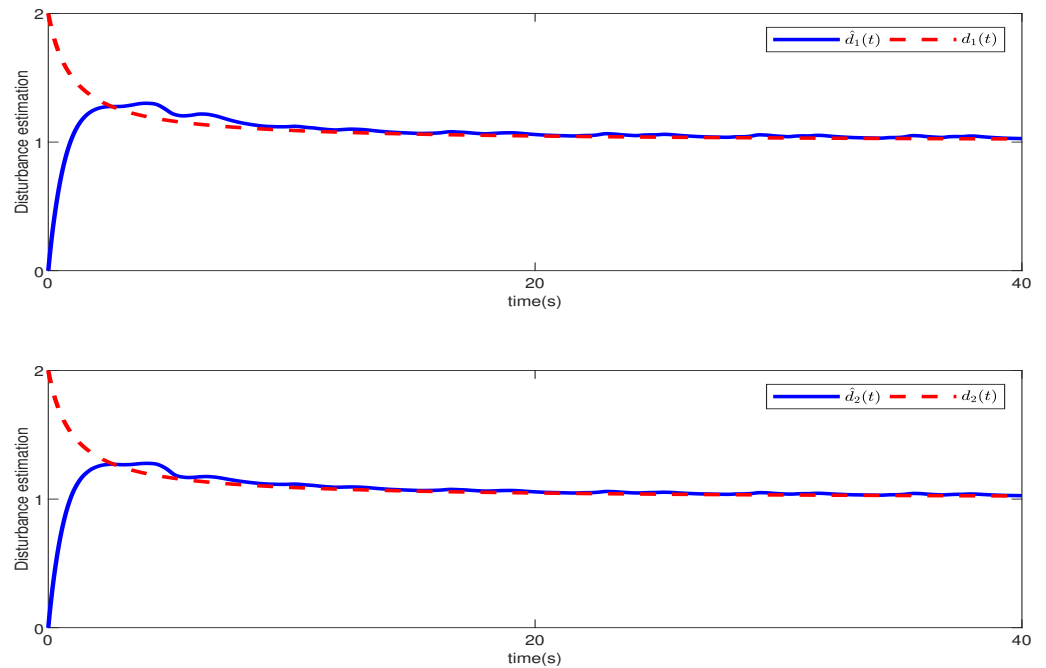


Figure 6. Disturbance estimation results.

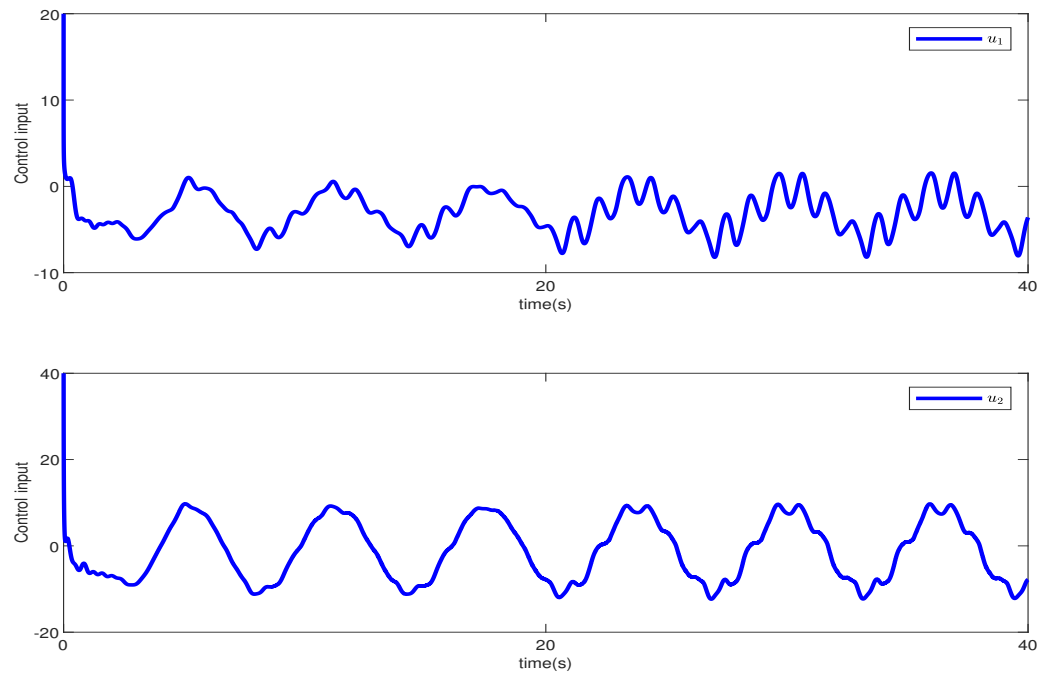


Figure 7. The responses of control inputs.

5. Conclusions

This paper focuses on addressing the issue of tracking control for n -link flexible-joint robot systems, considering both external disturbances and full-state constraints. To tackle this problem, we employ a transformation technique to convert the original dynamic system into a chained system. Additionally, a nonlinear disturbance observer is introduced to mitigate the impact of disturbances. Subsequently, the constrained system is transformed into an unconstrained system through SDF transformation, enabling the design of a tracking controller using the backstepping and filter technique. By appropriately selecting design parameters, we can ensure the stability of the resulting closed-loop system, adherence to the desired constraints, and a significant reduction in tracking errors. The proposed

method is validated through simulations performed on a two-link FJ manipulator system. Our future works will study the anti-disturbance control for other underactuated systems, such as underactuated crane systems [44–46].

Author Contributions: Conceptualization, Z.Z.; methodology, Z.Z.; validation, P.H.; writing—original draft preparation, X.H.; writing—review and editing, P.H. All authors have read and agreed to the published version of the manuscript.

Funding: This work was partly supported by the National Key Research and Development Program of China (2021YFE0193900), the National Natural Science Foundation of China (62173207), the China Postdoctoral Science Special Foundation (2023T160334), the Youth Innovation Team Project of Colleges and Universities in Shandong Province (2022KJ176), and the Graduate Teaching Case Base Project of Shandong Province (SDYAL20109).

Institutional Review Board Statement: Not applicable.

Data Availability Statement: No data were used to support this study.

Conflicts of Interest: The authors declare no conflicts of interest.

References

1. Wang, H.; Zhang, Y.; Zhao, Z.; Tang, X.; Yang, J.; Chen, I.-M. Finite-time disturbance observer-based trajectory tracking control for flexible-joint robots. *Nonlinear Dyn.* **2021**, *106*, 459–471. [\[CrossRef\]](#)
2. Ding, B.; Li, X.; Li, C.; Li, Y.; Chen, S.-C. A Survey on the mechanical design for piezo-actuated compliant micro-positioning stages. *Rev. Sci. Instrum.* **2023**, *94*, 10. [\[CrossRef\]](#)
3. Zhang, Q.; Zhao, X. Inverse dynamics modeling and simulation analysis of multi-flexible-body spatial parallel manipulators. *Electronics* **2023**, *12*, 2038. [\[CrossRef\]](#)
4. Jerbi, H.; Al-Darraj, I.; Tsaramirsis, G.; Kchaou, M.; Abbassi, R.; AlShammari, O. Fuzzy Luenberger observer design for nonlinear flexible joint robot manipulator. *Electronics* **2022**, *11*, 1569. [\[CrossRef\]](#)
5. Pană, C.; Vladu, C.; Pătrașcu-Pană, D.; Besnea, F.; Cismaru, Ç.; Trăsculescu, A.; Reșceanu, I.; Bizdoacă, N. Position control for hybrid infinite-continuous hyper-redundant robot. *Proc. MATEC Web Conf.* **2021**, *343*, 08009. [\[CrossRef\]](#)
6. Liu, Y.; Song, B.; Zhou, X.; Gao, Y.; Chen, T. An adaptive torque observer based on fuzzy inference for flexible joint application. *Machines* **2023**, *11*, 794. [\[CrossRef\]](#)
7. Krikochoritis, T.E.; Tzafestas, S.G. Control of flexible joint robots using neural networks. *IMA J. Math. Control Inf.* **2001**, *18*, 269–280. [\[CrossRef\]](#)
8. Yoo, S.J.; Choi, Y.H. Adaptive output feedback control of flexible-joint robots using neural networks: Dynamic surface design approach. *IEEE Trans. Neural Netw.* **2008**, *19*, 1712–1726.
9. Yoo, S.J.; Park, J.B.; Choi, Y.H. Adaptive dynamic surface control of flexible-joint robots using self-recurrent wavelet neural networks. *IEEE Trans. Syst. Man Cybern. B Cybern.* **2006**, *36*, 1342–1355. [\[CrossRef\]](#)
10. Zhang, Y.; Lei, Y.; Zhang, T.; Song, R.; Li, Y.; Du, F. Robust command-filtered control with prescribed performance for flexible-joint robots. *IEEE Trans. Instrum. Meas.* **2023**, *72*, 7506013. [\[CrossRef\]](#)
11. Yan, Y.-L.; Ding, L.; Ren, T.; Liu, F.-C. Research on backstepping control of flexible joint manipulator with state constraint. In Proceedings of the 2023 9th International Conference on Control, Automation and Robotics, Beijing, China, 21–23 April 2023; pp. 30–35.
12. Spong, M.; Khorasani, K.; Kokotovic, P. An integral manifold approach to the feedback control of flexible joint robots. *IEEE Trans. Robot. Autom.* **1987**, *3*, 291–300. [\[CrossRef\]](#)
13. Moallem, M.; Khorasani, K.; Patel, R.V. Tip position tracking of flexible multi-link manipulators: An integral manifold approach. In Proceedings of the IEEE International Conference on Robotics and Automation, Minneapolis, MN, USA, 22–28 April 1996; Volume 3, pp. 2432–2437.
14. Arefi, M.M.; Navid, V.; Behrouz, H.; Davoodi, M. Command filtered backstepping control of constrained flexible joint robotic manipulator. *IET Contr. Theory Appl.* **2023**, *17*, 2506–2518. [\[CrossRef\]](#)
15. Yang, K.; Zhao, L. Command-filter-based backstepping control for flexible joint manipulator systems with full-state constrains. *Int J. Control Autom. Syst.* **2022**, *20*, 2231–2238. [\[CrossRef\]](#)
16. Malki, H.A.; Misir, D.; Feigen span, D.; Chen, G. Fuzzy PID control of a flexible-joint robot arm with uncertainties from time-varying loads. *IEEE Trans. Control Syst. Technol.* **1997**, *5*, 371–378. [\[CrossRef\]](#)
17. Akyuz, I.H.; Yolacan, E.; Ertunc H.M.; Bingul, Z. PID and state feedback control of a single-link flexible joint robot manipulator. In Proceedings of the 2011 IEEE International Conference on Mechatronics, Istanbul, Turkey, 13–15 April 2011; pp. 409–414.
18. Wang, H.M.; Zhang, Z.Z.; Tang, X.L.; Zhao, Z.H.; Yan, Y.D. Continuous output feedback sliding mode control for underactuated flexible-joint robot. *J. Frankl. Inst.* **2022**, *359*, 7847–7865. [\[CrossRef\]](#)
19. Khan, R.F.; Rsetam, K.; Cao, Z.; Man, Z. Singular perturbation-based adaptive integral sliding mode control for flexible joint robots. *IEEE Trans. Ind. Electron.* **2023**, *70*, 10516–10525. [\[CrossRef\]](#)

20. Kang, S.; Liu, P.X.; Wang, H. Adaptive fuzzy finite-time command filtering control for flexible-joint robot systems against multiple actuator constraints. *IEEE Trans. Circuits Syst. II-Express Briefs* **2023**, *70*, 4554–4558. [[CrossRef](#)]
21. Zhu, Y.; Liu, J.; Wang, Q.G. Command filtering-based adaptive fuzzy control of flexible-joint robots with time-varying full-state constraints. *IEEE Trans. Circuits Syst. II-Express Briefs* **2024**, *71*, 682–686. [[CrossRef](#)]
22. Li, T.; Li, Z.; Wang, D.; Chen, C.L.P. Output-feedback adaptive neural control for stochastic nonlinear time-varying delay systems with unknown control directions. *IEEE Trans. Neural Netw. Learn. Syst.* **2015**, *26*, 1188–1201. [[CrossRef](#)]
23. Liu, Z.; Lai, G.; Zhang, Y.; Chen, X.; Chen, C.L.P. Adaptive neural control for a class of nonlinear time-varying delay systems with unknown hysteresis. *IEEE Trans. Neural Netw. Learn. Syst.* **2014**, *25*, 2129–2140.
24. Diao, S.Z.; Sun, W.; Su, S.F. Neural-based adaptive event-triggered tracking control for flexible-joint robots with random noises. *Int. J. Robust Nonlinear Control* **2022**, *32*, 2722–2740. [[CrossRef](#)]
25. Yang, X.; Sun, W.; Dong, H.; Wu, X. Adaptive prescribed performance fuzzy Control for n -Link flexible-joint robots under event-triggered mechanism. *Int. J. Fuzzy Syst.* **2023**, *25*, 1019–1033. [[CrossRef](#)]
26. Guo, Y.; Hou, Z.; Liu, S.; Jin, S. Data-driven model-free adaptive predictive control for a class of MIMO nonlinear discrete-time systems with stability analysis. *IEEE Access* **2019**, *7*, 102852–102866. [[CrossRef](#)]
27. Luo, W.; Lu, P.; Liu, H.; Du, C. Event-triggered networked predictive output tracking control of cyber-physical systems with model uncertainty and communication constraints. *IEEE Trans. Circuits Syst. II-Express Briefs* **2023**, *70*, 2166–2170. [[CrossRef](#)]
28. Lv, M.; Yu, W.; Baldi, S. The set-invariance paradigm in fuzzy adaptive DSC design of large-scale nonlinear input-constrained systems. *IEEE Trans. Syst. Man Cybern.-Syst.* **2021**, *51*, 1035–1045. [[CrossRef](#)]
29. Nguyen, A.T.; Rath, J.; Guerra, T.M.; Palhares, R.; Zhang, H. Robust set-invariance based fuzzy output tracking control for vehicle autonomous driving under uncertain lateral forces and steering constraints. *IEEE Trans. Intell. Transp. Syst.* **2021**, *22*, 5849–5860. [[CrossRef](#)]
30. Liu, Y.J.; Li, J.; Tong, S.; Chen, C.L.P. Neural network control-based adaptive learning design for nonlinear systems with full-state constraints. *IEEE Trans. Neural Netw. Learn. Syst.* **2016**, *27*, 1562–1571. [[CrossRef](#)]
31. Liu, L.; Cui, Y.; Liu, Y.J.; Tong, S. Adaptive event-triggered output feedback control for nonlinear switched systems based on full state constraints. *IEEE Trans. Circuits Syst. II-Express Briefs* **2022**, *69*, 3779–3783. [[CrossRef](#)]
32. Liu, A.; Li, H. Stabilization of delayed boolean control networks with state constraints: a barrier Lyapunov function method. *IEEE Trans. Circuits Syst. II-Express Briefs* **2021**, *68*, 2553–2557. [[CrossRef](#)]
33. Sun, W.; Su, S.F.; Xia, J.; Nguyen, V.-T. Adaptive fuzzy tracking control of flexible-joint robots with full-state constraints. *IEEE Trans. Syst. Man Cybern. Syst.* **2019**, *49*, 2201–2209. [[CrossRef](#)]
34. Feng, Y.; Kong, L.; Zhang, Z.; Liu, R.; Cheng, G.; Yu, X. Event-triggered finite-time control for a constrained robotic manipulator with flexible joints. *Int. J. Robust Nonlinear Control* **2023**, *33*, 6031–6051. [[CrossRef](#)]
35. Tian, L.R.; Gao, Y.; Zhang, Z.C. Disturbance-observer-based tracking controller for a flexible-joint robotic manipulator with full-state constraints. *Proc. Inst. Mech. Eng. Part I J. Syst. Control. Eng.* **2022**, *236*, 1166–1175. [[CrossRef](#)]
36. Chen, W.H.; Ballance, D.J.; Gawthrop, P.J.; O'Reilly, J. A nonlinear disturbance observer for robotic manipulators. *IEEE Trans. Ind. Electron.* **2000**, *47*, 932–938. [[CrossRef](#)]
37. Ma, H.; Ren, H.; Zhou, Q.; Li, H.; Wang, Z. Observer-based neural control of n -link flexible-joint robots. *IEEE Trans. Neural Netw. Learn. Syst.* **2024**, *35*, 5295–5305. [[CrossRef](#)] [[PubMed](#)]
38. Sun, T.R.; Cheng, L.; Wang, W.Q.; Pan, Y. Semiglobal exponential control of Euler-Lagrange systems using a sliding-mode disturbance observer. *Automatica* **2020**, *112*, 108677. [[CrossRef](#)]
39. Wen, Q.; Yang, X.; Huang, C.; Zeng, J.; Yuan, Z.; Liu, P.X. Disturbance observer-based neural network integral sliding mode control for a constrained flexible joint robotic manipulator. *Int. J. Control Autom. Syst.* **2023**, *21*, 1243–1257. [[CrossRef](#)]
40. Diao, S.; Sun, W.; Su, S.-F.; Xia, J. Adaptive fuzzy event-triggered control for single-link flexible-joint robots with actuator failures. *IEEE Trans. Cybern.* **2022**, *52*, 7231–7241. [[CrossRef](#)] [[PubMed](#)]
41. Cao Y.; Song Y.D.; Wen C.Y. A unified event-triggered control approach for uncertain pure-feedback systems with or without state constraints. *IEEE Trans. Syst. Man Cybern. Syst.* **2021**, *51*, 1262–1271. [[CrossRef](#)] [[PubMed](#)]
42. Ding, B.; Li, Y. Hysteresis compensation and sliding mode control with perturbation estimation for piezoelectric actuators. *Micromachines* **2018**, *9*, 241. [[CrossRef](#)]
43. Ling, S.; Wang, H.; Liu, P. X. Adaptive fuzzy tracking control of flexible-joint robots based on command filtering. *IEEE Trans. Ind. Electron.* **2019**, *67*, 4046–4055. [[CrossRef](#)]
44. Feng, Y.A.; Zhang, H.; Gu, C. The prescribed-time sliding mode control for underactuated bridge crane. *Electronics* **2024**, *13*, 219. [[CrossRef](#)]
45. Yu, Z.A.; Niu, W.Q. Flatness-based backstepping antisway control of underactuated crane systems under wind disturbance. *Electronics* **2023**, *12*, 244. [[CrossRef](#)]
46. Abbasimoshaei, A.; Chinnakkonda Ravi A.K.; Kern T.A. Development of a new control system for a rehabilitation robot using electrical impedance tomography and artificial intelligence. *Biomimetics* **2023**, *8*, 420. [[CrossRef](#)] [[PubMed](#)]

Disclaimer/Publisher's Note: The statements, opinions and data contained in all publications are solely those of the individual author(s) and contributor(s) and not of MDPI and/or the editor(s). MDPI and/or the editor(s) disclaim responsibility for any injury to people or property resulting from any ideas, methods, instructions or products referred to in the content.